Supramolecular Networks Using Ferrocenyl Ditriazole and Diimidazole Bridges

Ye Gao, Brendan Twamley, and Jean'ne M. Shreeve*

Department of Chemistry, University of Idaho, Moscow, Idaho 83844-2343

Supramolecular coordination networks showing redox activity were obtained by reacting ferrocene-based bidentate ligands, 1,1′-bis[(1*H*-1,2,4-triazol-1-yl)methyl]ferrocene (**1**) and 1,1′-bis{[1*H*-(2-methyl)-imidazol-1-yl]methyl}ferrocene (**2**), with AgNO$_3$, CdCl$_2$, and ZnCl$_2$ using a layering technique. The resulting extended networks display a variety of different conformations, which highlights the flexibility of the bridging ligand: **1**·AgNO$_3$ (**3**), 1-D helical array; **1**$_2$·CdCl$_2$ (**4**), 1-D cross-linked network; **1**·ZnCl$_2$ (**5**), 1-D zigzag array; and **2**·ZnCl$_2$ (**6**), 1-D zigzag array.

Introduction

Construction of mixed-metal superstructures and the design of supramolecular species are areas of contining interest.[1] Our desire is to exploit the topological and electronic properties of metal centers to construct supramolecular materials in which metal centers communicate via coordination bonds or other noncovalent interactions.[2] The engineering of the metal center linkage via organic ligands is at the core of this booming field of coordination network chemistry.[3,4] We aim to apply supramolecular chemistry approaches to organometallic chemistry, while focusing on crystal engineering strategies.[5]

The versatile ferrocene molecule has found renewed applications in materials chemistry, organic synthesis, and catalysis.[6−8] Several groups have reported the synthesis of ferrocene-based bidentate ligands that contain pyridine and rigid or flexible spacers −CH$_2$−, −S−, −N=N−, etc., and their interesting coordination complexes.[9] Pyridyl-based bridging ferrocene ligands have proved to be highly effective metal linkers. However, these species are not always ideal candidates for supramolecular coordination networks, and most ligands tend to give chelate or *molecular* compounds.

In this paper, we describe the use of bidentate ferrocene ligands **1**, 1,1′-bis[(1*H*-1,2,4-triazol-1-yl)methyl]ferroecene, and **2**, 1,1′-bis{[1*H*-(2-methyl)imidazol-1-yl]methyl}ferrocene, as self-assembly supramolecular agents. The reaction of these ligands with metal salts, such as Ag^{I}NO$_3$, Cd^{II}Cl$_2$, and Zn^{II}Cl$_2$, yields the supramolecular coordination networks **1**·AgNO$_3$ (**3**), **1**$_2$·CdCl$_2$ (**4**), **1**·ZnCl$_2$ (**5**), and **2**·ZnCl$_2$ (**6**) (Scheme 1).

Results

(a) Structure. Our preparation of the bidentate ferrocene ligands **1** and **2** has been described previously.[10] These ligands were reacted with the metal salts AgNO$_3$, CdCl$_2$, and ZnCl$_2$ via layering a methanol solution of the ligand onto a water solution of metal salt in a test tube at room temperature. Compounds **3**−**6** are air- and moisture-stable yellow crystalline materials. With the exception of **3**, these compounds did not dissolve in common solvents such as acetone, acetonitrile, methanol, methylene chloride, DMF, and DMSO. Compound **3** partially dissolves in acetonitrile.

General Structural Description. Compounds **3**−**6** are all supramolecular arrays with metal-organic frameworks (MOF). Apart from compound **4**, all are one-dimensional chainlike arrays with the metal salt coordinating to the linking tri- or diazole. Each has unique structural architecture imposed by the metal coordination and characterized by additional metal interactions as well as hydrogen bonding (vide infra). Compound **4** has a different structural motif imposed by the octahedral coordination of cadmium. In this case, two ligands bridge different Cd centers, forming a "wide" chain array. The single-

---

* To whom correspondence should be addressed. E-mail: jshreeve@uidaho.edu.

(1) (a) Haiduc, I.; Edelmann, F. T. *Supramolecular Organometallic Chemistry*; Wiley-VCH: Weinheim, 1999. (b) Steed, J. W.; Atwood, J. L. *Supramolecular Chemistry*; Wiley & Sons: Chichester, 2000.

(2) (a) Braga, D.; Grepioni, F. *Acc. Chem. Res.* **2000**, *33*, 601−608. (b) Garcia, A. M.; Bassani, D. M.; Lehn, J. M.; Baum, G.; Fenske, D. *Chem. Eur. J.* **1999**, *5*, 1234−1238.

(3) (a) Eddaouddi, M.; Moler, D. B.; Li, H.; Chen, B.; Reineke, T. M.; O'Keeffe, M.; Yaghi, O. M. *Acc. Chem. Res.* **2001**, *34*, 319−330. (b) Batten, S. R. *CrystEngComm* **2001**, *3*, 67−73.

(4) *J. Chem. Soc., Dalton Trans.* **2000**, 3705−3998 (entire issue).

(5) (a) Braga, D.; Grepioni, F.; Desiraju, G. R. *Chem. Rev.* **1998**, *98*, 1375−1406. (b) Braga, D.; Grepioni, F. *Coord. Chem. Rev.* **1999**, *183*, 19−41.

(6) Long, N. J. *Metallocenes*; Blackwell: Oxford, 1998.

(7) *Metallocenes*; Togni, A., Halterman, R. L., Eds.; VCH: Weinheim, 1998.

(8) *Ferrocene, Homogeneous Catalysis, Organic Synthesis and Materials Science*; Togni, A., Hayashi, T., Eds.; VCH: Weinheim, 1995.

(9) (a) Horikoshi, R.; Mochida, T.; Moriyama, H. *Inorg. Chem.* **2002**, *41*, 3017−3024. (b) Barranco, E. M.; Crespo, O.; Gimeno, M. C.; Jones, P. G.; Laguna, A.; Sarroca, C. *J. Chem. Soc., Dalton Trans.* **2001**, 2523−2529. (c) Hou, H.; Li, L.; Zhu, Y.; Fan, Y.; Qiao, Y. *Inorg. Chem.* **2004**, *43*, 4767−4774. (d) Fang, C.; Duan, C.; Guo, D.; He, C.; Meng, Q.; Wang, Z.; Yan, C. *Chem. Commun.* **2001**, 2540−2541. (e) Braga, D.; Polito, M.; Bracaccini, M.; D'Addario, D.; Tagliavini, E.; Proserpio, D. M.; Grepioni, F. *Chem. Commun.* **2002**, 1080−1081. (f) Lindner, E.; Zong, R.; Eichele, K.; Weisser, U.; Ströbele, M. *Eur. J. Inorg. Chem.* **2003**, 705−712. (g) Ion, A.; Moutet, J.-C.; Saint-Amam, E.; Royal, G.; Tingry, S.; Pecaut, J.; Menage, S.; Ziessel, R. *Inorg. Chem.* **2001**, *40*, 3632−3636. (h) Buda, M.; Moutet, J.-C.; Saint-Aman, E.; Cian, A. D.; Fischer, J.; Ziessel, R. *Inorg. Chem.* **1998**, *37*, 4146−4148. (i) Fang, C.; Duan, C.; Mo, H.; He, C.; Meng, Q.; Liu, Y.; Mei, Y.; Wang, Z. *Organometallics* **2001**, *20*, 2525−2532. (j) Tani, K.; Mihana, T.; Yamagata, T.; Saito, T. *Chem. Lett.* **1991**, 2047−2050. (k) Neumann, B.; Siemeling, U.; Stammler, H.-G.; Vorfeld, U.; Delis, J. G. P.; Leeuwen, P. W. N. M.; Vrieze, K.; Fraanje, J.; Goubitz, K.; Biani, F. F.; Zanello, P. *J. Chem. Soc., Dalton Trans.* **1997**, 4705−4711. (l) Reger, D. L.; Brown, K. J.; Gardinier, J. R.; Smith, M. D. *J. Organomet. Chem.* **2005**, *690* (8), 1889−1900. (m) Ilkhechi, A. H.; Bolte, M.; Lerner, H. W.; Wagner, M. *J. Organomet. Chem.* **2005**, *690* (8), 1971−1977.

(10) Gao, Y.; Twamley, B.; Shreeve, J. M. *Inorg. Chem.* **2004**, *43*, 3406−3412.

Table 1. Crystallographic Data for 3−6

	3	4	5	6
formula	$C_{16}H_{16}Ag\ FeN_7O_3$	$C_{32}H_{32}CdCl_2Fe_2N_{12}$	$C_{16}H_{16}Cl_2FeN_6Zn$	$C_{20}H_{22}Cl_2FeN_4Zn$
exposure (s)	5	10	5	40
fw	518.08	879.70	484.47	510.54
cryst size (mm)	$0.22 \times 0.08 \times 0.03$	$0.21 \times 0.07 \times 0.06$	$0.41 \times 0.41 \times 0.14$	$0.21 \times 0.14 \times 0.02$
cryst syst	monoclinic	triclinic	triclinic	monoclinic
space group	$C2/c$	$P\bar{1}$	$P\bar{1}$	$C2/c$
a (Å)	22.2379(11)	7.0577(3)	7.3608(4)	14.902(1)
b (Å)	7.6304(4)	8.5381(4)	11.1924(6)	11.6328(8)
c (Å)	10.6537(5)	15.1071(6)	12.0129(6)	13.340(1)
α (deg)	90	98.342(1)	71.008(1)	90
β (deg)	105.292(1)	92.997(1)	75.759(1)	117.339(1)
γ (deg)	90	112.781(1)	84.464(1)	90
V (Å³)	1743.76(15)	824.56(6)	906.91(8)	2054.3(3)
D_c (Mg m⁻³)	1.973	1.772	1.774	1.651
Z	4	1	2	4
μ (mm⁻¹)	1.991	1.715	2.430	2.147
total no. of reflns	12 682	12 320	13 387	13 577
R(int)	0.0301	0.0305	0.0203	0.0529
no. of data/restraints/params	1987/27/123	3769/0/223	4180/0/238	2368/0/130
index ranges	$-28 \le h \le 28,$	$-9 \le h \le 9,$	$-9 \le h \le 9,$	$-19 \le h \le 19,$
	$-9 \le k \le 9,$	$-11 \le k \le 11,$	$-14 \le k \le 14,$	$-15 \le k \le 15,$
	$-13 \le l \le 13$	$-19 \le l \le 19$	$-15 \le l \le 15$	$-17 \le l \le 17$
$F(000)$	1032	442	488	1040
R1, wR2 ($I > 2\sigma(I)$)[a]	0.0294, 0.0651	0.0290, 0.0648	0.0211, 0.0539	0.0370, 0.0780
R1, wR2 (all data)[a]	0.0310, 0.0659	0.0327, 0.0664	0.0221, 0.0545	0.0508, 0.0828
GOF on F^2	1.040	1.050	1.024	1.092
$\Delta\rho_{min}, \Delta\rho_{max}$ (e Å⁻³)	0.637, −0.657	0.886, −0.389	0.386, −0.264	0.843, −0.543

[a] $R_1 = \sum||F_o| - |F_c||/\sum|F_o|$. $wR_2 = [\sum(w|F_o^2 - F_c^2|^2)/\sum w|F_o^2|^2]^{1/2}$.

Table 2. Selected Bond Lengths [Å] and Angles [deg] for 3−6[a]

3

Ag(1)−N(10B)^i	2.144(6)	Ag(1)−N(10B)^{ii}	2.144(6)
Ag(1)−N(10)	2.149(7)	Ag(1)−N(10)^{iii}	2.149(7)
N(10B)^i−Ag(1)−N(10B)^{ii}	157.2(4)	N(10B)^i−Ag(1)−N(10)	6.5(3)
N(10B)^{ii}−Ag(1)−N(10)	151.9(2)	N(10B)^i−Ag(1)−N(10)^{iii}	151.9(2)
N(10B)^{ii}−Ag(1)−N(10)^{iii}	6.5(3)	N(10)−Ag(1)−N(10)^{iii}	147.4(4)
N(7)−C(6)−C(5)	110.8(4)	N(7B)−C(6B)−C(5B)	110.8(5)

4

Cd(1)−N(10)	2.3138(19)	Cd(1)−N(10)^i	2.3138(19)
Cd(1)−N(21)^{ii}	2.3876(19)	Cd(1)−N(21)^{iii}	2.3876(19)
Cd(1)−Cl(1)^i	2.6162(5)	N(21)−Cd(1)^{iv}	2.3876(19)
N(10)−Cd(1)−N(10)^i	180.0	N(10)−Cd(1)−N(21)^{ii}	86.69(7)
N(10)^i−Cd(1)−N(21)^{ii}	93.31(7)	N(10)−Cd(1)−N(21)^{iii}	93.31(7)
N(10)^i−Cd(1)−N(21)^{iii}	86.69(7)	N(21)^{ii}−Cd(1)−N(21)^{iii}	180.000(1)
N(10)−Cd(1)−Cl(1)^i	91.59(5)	N(10)^i−Cd(1)−Cl(1)^i	88.41(5)
N(21)#2−Cd(1)−Cl(1)^i	93.92(5)	N(21)^{iii}−Cd(1)−Cl(1)^i	86.08(5)
N(10)−Cd(1)−Cl(1)	88.41(5)	N(10)^i−Cd(1)−Cl(1)	91.59(5)
N(21)^{ii}−Cd(1)−Cl(1)	86.08(5)	N(21)^{iii}−Cd(1)−Cl(1)	93.92(5)
Cl(1)^i−Cd(1)−Cl(1)	180.0		
N(7)−C(6)−C(5)	111.37(18)	N(18)−C(17)−C(16)	114.25(19)

5

Zn−N(10)	2.029(13)	Zn−N(12)	2.018(12)
Zn−Cl(1)	2.221(4)	Zn−Cl(2)	2.235(4)
N(10)−Zn−N(12)	100.28(5)	N(12)−Zn−Cl(1)	114.71(4)
N(10)−Zn−Cl(1)	105.71(4)	N(12)−Zn−Cl(2)	107.89(4)
N(10)−Zn−Cl(2)	116.11(4)	Cl(1)−Zn−Cl(2)	111.83(15)
N(7)−C(6)−C(5)	113.41(12)	N(15)−C(17)−C(18)	112.44(12)

6

Zn−N(9)	2.024(2)	Zn−N(9)^{ii}	2.024(2)
Zn−Cl(1)^{ii}	2.247(7)		
N(9)^{ii}−Zn−N(9)	102.80(12)	N(9)^{ii}−Zn−Cl(1)^{ii}	104.21(7)
N(9)−Zn−Cl(1)^{ii}	114.85(6)	Cl(1)−Zn−Cl(1)^{ii}	115.51(4)
N(7)−C(6)−C(5)	112.7(2)		

[a] Symmetry transformations used to generate equivalent atoms: **3**: i $-x + 1/2, -y + 5/2, -z + 1$, ii $x + 1/2, -y + 5/2, z - 1/2$, iii $-x + 1, y, -z + 1/2$; **4**: i $-x + 2, -y, -z + 1$, ii $x + 1, y - 1, z$, iii $-x + 1, -y + 1, -z + 1$, iv $x - 1, y + 1, z$; **6**: ii $-x + 2, y, -z + 1/2$.

crystal X-ray structural data are presented in Table 1. Selected bond lengths and angles are given in Table 2.

[Ag{1,1′-bis[(1H-1,2,4-triazol-1-yl)methyl]ferrocene}N-O₃]$_n$ (3). Crystallographically this compound displays whole molecule disorder (see Experimental Section and Supporting Information). The one-dimensional supramolecular conformation forms a helical array accompanied with chelated NO₃ anions at the Ag centers (Figure 1a). The helical repeat is two and the arrangement of ligand **1** is *trans*, with the triazole rings tilted ca. 70° to the ferrocene ring. The silver is two-coordinate with an angle of 157.2(4)° (Table 2) to each ligand. However, the triazoles and Ag atom are coplanar. There are a variety of weak nonclassical hydrogen bonds between the chain and the nitrate anion (C−H···O 2.9−3.16 Å). The helices are tied together via Ag···O intermolecular interactions. There is a bifurcated O1a···Ag···O interaction of 2.739 Å (vdW, 3.24 Å) and a longer single Ag···O2 (3.259 Å) interaction to the next nitrate group, which in turn has strong interactions with the next Ag center. This binds the helical arrays into a loosely bound sheet, with the arrays packed in a staggered fashion (Figure 1b).

[Cd{1,1′-bis[(1H-1,2,4-triazol-1-yl)methyl]ferrocene}₂C-l₂]$_n$ (4). Each Cd center in **4** is six-coordinate. Four ligands, **1**, are coordinated equatorially to each CdCl₂ center, forming a twisted double-chain array (Figure 2a). The deviation from octahedral coordination is small, with N−Cd−Cl angles of 86−93.9° and N−Cd−N and Cl−Cd−Cl angles of 180° (see Table 2). In this array the triazoles are arranged in a pseudo-*cis* fashion around the ferrocene, leading to a "puckered" or twisted chain. The void in each link is occupied by the halide of the next chain, forming weak C−H···Cl interactions (ca. 3.6 Å). A small segment of the packing is shown in Figure 2b.

[Zn{1,1′-bis[(1H-1,2,4-triazol-1-yl)methyl]ferrocene}Cl₂]$_n$ (5). In this array, the Zn atom has distorted tetrahedral coordination (Figure 3a). There are two ligands, **1**, coordinated to the ZnCl₂ moiety (N−Zn−N = 100.28(5)°; Cl−Zn−Cl = 111.83(15)°; Table 2). The ligand, in this case as in **3**, is oriented in a pseudo-*trans* orientation about the ferrocene. The triazole ring plane is canted at ca. 63° to the plane of the ferrocene ring, and both triazoles on either side of the ferrocene are parallel. This leads to a zigzag chain formation, resulting in a close packing arrangement (Figure 3b). There are nonclassical hydrogen bonds between each strand (C9−H9···C12, 3.52 Å;
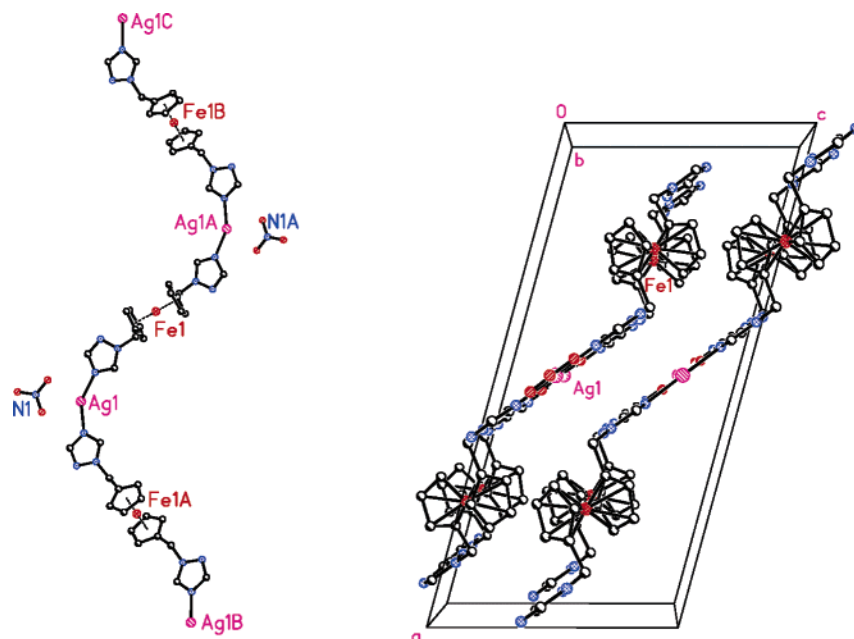
Figure 1. (a) Illustration of **3** showing the helix repeat; (b) packing diagram of **3** viewed down the *b* axis showing the unit cell and the parallel packing of the helical arrays. Hydrogen atoms are omitted for clarity.
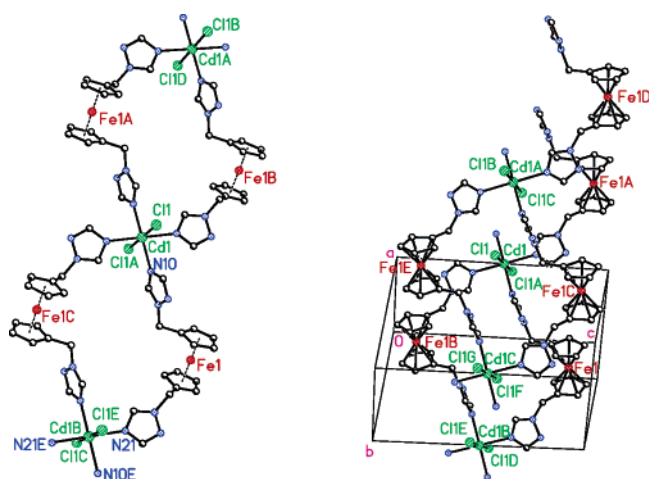

Figure 2. (a) Illustration of the double ligand twisted chain in **4**; (b) section of the packing of **4** showing the overlapping chains. Hydrogen atoms are omitted for clarity.

C11−H11···N14, 3.42 Å; C16−H16···N8, 3.48 Å), resulting in a weakly associated 3-D network.

[Zn[1,1′-bis{[1-(2-methyl)imidazol-1-yl]methyl}ferrocene]-Cl₂]ₙ (6). Reaction of ZnCl₂ with type **2** ligands led to a different
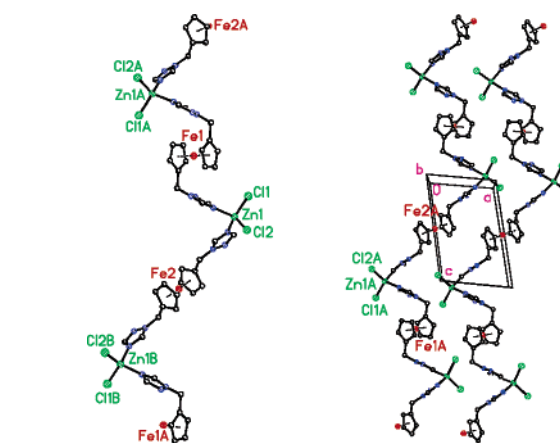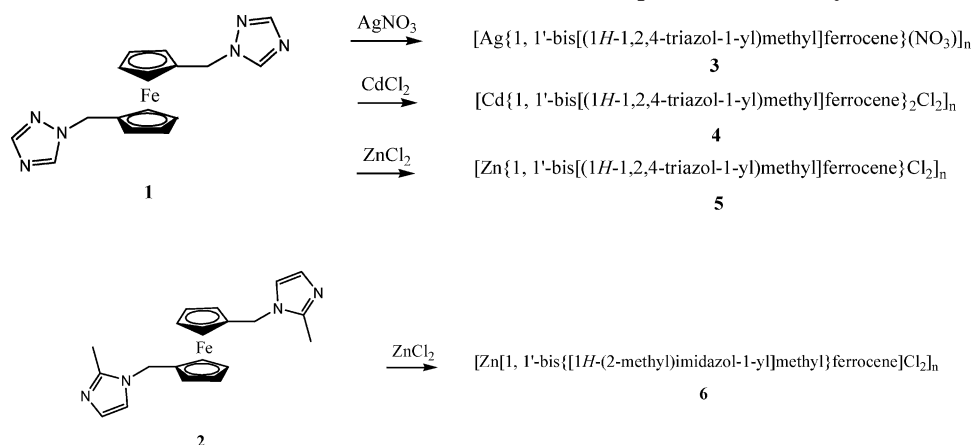

Figure 3. (a) Illustration of the array in **5**; (b) supramolecular structure of **5** showing the close packing of the arrays.

array. The Zn center still has a distorted tetrahedral coordination with angles Cl−Zn−Cl, 115.51 (4)°, and N−Zn−N, 102.80 (12)° (Table 2). The imidazole groups are arranged in the *trans* orientation and each methyl imidazolium group is also *trans* to the other (see Figure 4a). This leads to an alternating parallelepiped type arrangement of the metal and ligand framework

Scheme 1. Reaction Scheme for the Formation of Supramolecular Arrays 3−6

[Ag{1, 1'-bis[(1*H*-1,2,4-triazol-1-yl)methyl]ferrocene}(NO₃)]ₙ

3

[Cd{1, 1'-bis[(1*H*-1,2,4-triazol-1-yl)methyl]ferrocene}₂Cl₂]ₙ

4

[Zn{1, 1'-bis[(1*H*-1,2,4-triazol-1-yl)methyl]ferrocene}Cl₂]ₙ

5

[Zn[1, 1'-bis{[1*H*-(2-methyl)imidazol-1-yl]methyl}ferrocene]Cl₂]ₙ
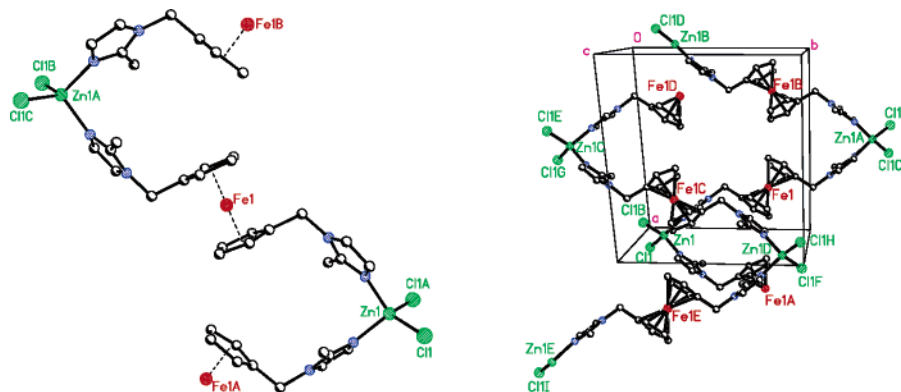
6

Figure 4. (a) Illustration of the structure repeat in **6**; (b) section of the packing in **6** showing the channel formed parallel to the *c* axis. Only metal and halide atoms are labeled and H atoms are omitted for clarity.
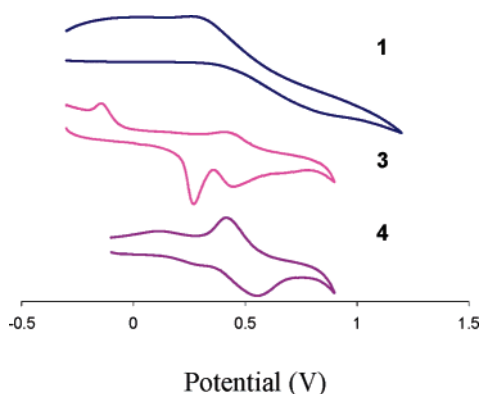

Potential (V)

Figure 5. Solid-state cyclic voltammograms (Ag/AgCl reference electrode) of complexes **1**, **3**, and **4**.

Table 3. Solid-State Redox Potentials from Cyclic Voltammetry (reference Ag/AgCl electrode)

	E_{pa} (V)	E_{pc} (V)
1	0.87[a]	0.26[a]
2	0.62	0.46
3	0.46, 0.27[a]	0.40, −0.14[a]
4	0.55	0.42
5	0.55	0.37
6	0.59	0.49

[a] Independent irreversible waves.

governed by the methylene and Zn angles (C5−C6−N7, 112.7-(2)°; N9−Zn1−N9, 102.8(1)°). The framework voids are all aligned in the packing diagram (Figure 4b), are approximately 5.5 Å^2, and are parallel to the *c* axis. In effect, these arrays are 1-D, as there are only two weak nonclassical hydrogen bonds between the ligand and the chlorine atoms of a neighboring array (C6⋯Cl1, 3.759(3) Å; C4⋯Cl1, 3.645(3) Å).

(b) Solid-State Redox Properties of 1−6. The insolubility of the complexes **3**−**6** implied that only solid-state cyclic voltammetry could be used to study their electrochemical behavior. Initial studies show that all complexes have an electrochemical response, and solid-state cyclic voltammograms of **1**, **3**, and **4** are shown in Figure 5, with redox potentials listed in Table 3.

The cyclic voltammograms of ligand **1** showed there were two independent irreversible oxidative and reductive waves, E_{pa} and E_{pc} at 0.87 and 0.26 V, respectively. The voltammograms of ligand **2** are similar to complexes **4**−**6** (see Table 3, vide infra), and these reversible peaks can be attributed to the ferrocene redox process. The behavior of compound **3** is more complex: there are two redox processes, a quasi-reversible process that corresponds to the ferrocene moiety and an

irreversible oxidative and reductive process with $E_{pa} = 0.27$ V and $E_{pc} = -0.14$ V.

Discussion

1,1′-Bis[(1*H*-1,2,4-triazol-1-yl)methyl]ferrocene (**1**) and 1,1′-bis{[1*H*-(2-methyl)imidazol-1-yl]methyl}ferrocene (**2**) were synthesized according to literature procedures, which involved the addition of azole (imidazole or triazole) to [FcCH₂{NCH₃)₃}₂]⋅2[I] (Fc = ferrocene).[10] This synthesis produces high yields (>90%), and various substitutions of the azole rings can also be accommodated for future ligand "tuning". The synthesis of the coordination polymers is relatively straightforward via the layering of a methanol solution of the ligand onto a water solution of the metal salt. The colored crystals of the products formed slowly over the course of days at the interface.

The design of the ligand as an integral supramolecular self-assembly unit depends on three critical factors: (a) bis-substitution, (b) a spacer between the azole and the ferrocene, and (c) conformational flexibility. There are few ferrocene-containing "ligands" that form supramolecular species instead of molecular or macromolecular units. Monosubstituted N-donor-substituted (e.g., pyridyl, pyrazyl) ligands abound, and metal complexes using these types of ligand produce mainly molecular species e.g., chloro(4-ferrocenylpyridine)(1,4,8,11-tetrathiacyclotetradecane)ruthenium(II) chloride ethanol solvate hydrate[11] and bis(3-ferrocenylpyrazine)dinitratocopper(II).[12] The exception to this are pyrimidine-substituted ferrocenes, which form supramolecular species, e.g., catena(bis(μ₂-5-ferrocenylpy-rimidine)tetrakis(1,1,1,5,5,5-hexafluoroacetylacetonato)dicopper-(II)).[13] These compounds, however, do not integrate the ferrocene moieties into the supramolecular array. Bis-substitution does not guarantee a supramolecular synthon. Ligands such as 1,1′-bis(2-pyridyl)ferrocene[9e,j,k] and 1,1′-bis(4-pyridyl)ferrocene yield molecular compounds,[9e,14] e.g., bis(μ₂-1,1′-bis(4-pyridyl)-ferrocene)tetrachlorodizinc(II) or bis(μ₂-1,1′-bis(4-pyridyl)fer-rocene)bis(μ₂-nitrato-*O,O*)methoxydinitratodicadmium(II) ben-zene solvate. The addition of a spacer also does not have to lead to a supramolecular species, e.g., the ligand bis(2-(3-

(11) Nunes, C. D.; Santos, T. M.; Carapuca, H. M.; Hazell, A.; Pillinger, M.; Madureira, J.; Xue, W. M.; Kühn, F. E.; Gonçalves, I. S. *New J. Chem.* **2002**, *26*, 1384−1388.

(12) Horikoshi, R.; Nambu, C.; Mochida, T. *Inorg. Chem.* **2003**, *42*, 6868−6875.

(13) Horikoshi, R.; Ueda, M.; Mochida, T. *New J. Chem.* **2003**, *27*, 933−937.

(14) Braga, D.; Polito, M.; D'Addario, D.; Tagliavini, E.; Proserpio, D. M.; Grepioni, F.; Steed, J. W. *Organometallics* **2003**, *22*, 4532−4538.

pyridyl)ethynyl)ferrocene), but can also lead to molecular compounds, e.g., bis(μ_2-1,1′-bis(2-(3-pyridyl)ethynyl)ferrocene-*N*,*N*′)disilver diperchlorate acetonitrile solvate.[9f] This ligand does not have the conformational flexibility needed to form a supramolecular species.

However, when the spacer is replaced with a sulfur atom, e.g., 1,1′-(4-dipyridinethio)ferrocene or 1,1′-(2-dipyridinethio)-ferrocene, a variety of supramolecular coordination polymers are obtained in both cases similar to **3**.[9a] Hence the conformational flexibility of this spacer is vital for linkage to metals with different coordinating capabilities. This criterion is clearly evident in compounds **3**−**6**, where ligand **1** or **2** adopts a range of conformations, with both azole substituents *trans* in **3** and **6**, pseudo-*trans* in **5**, and pseudo-*cis* in complex **4**.

Preliminary electrochemical results show that all complexes display redox behavior. Due to their poor solubility, solid-state cyclic voltammetry was used with a Ag/AgCl reference electrode. Given the conditions, ligand **1** shows an irreversible redox couple, and ligand **2** has a quasi-reversible wave couple. Although the reasons behind the irreversible couple are not clear yet, solid-state effects and chemical reactions can be factors in these measurements. The majority of the metal complexes show quasi-reversible couples at anodic potentials of ca. 550 mV and cathodic potentials of 430 mV, with an average $E_{1/2}$ of 490 mV, which can be attributed to the ferrocene/ferrocenium (Fc/Fc$^+$) couple, as seen in ligand **2** ($E_{1/2} = 540$ mV). These $E_{1/2}$ potentials are shifted relative to solution cyclic voltammetry of the Fc/Fc$^+$ couple ($E_{1/2} = 350$ mV vs Ag/AgCl). Other ferrocene derivatives however also demonstrate this type of shift in reversible oxidation, e.g., acetylferrocene ($E_{1/2} = 580$ mV vs Ag/AgCl). Compound **3** has unusual redox behavior. It has the quasi-reversible Fc/Fc$^+$ wave ($E_{1/2} = 430$ mV) but another irreversible couple with $E_{pa} = 270$ mV and $E_{pc} = -140$ mV. The origin of this potential is still unclear, but we suspect that this is a reaction leading to decomposition and Ag metal deposition.

Conclusion

In this paper we have shown that preformed organometallic ligands **1** and **2** with supramolecular bonding capacity can be used to prepare novel mixed-metal complexes in which the flexible ferrocenyl ligands take advantage of the conformational freedom around the metal center to form extended networks rather than finite complexes. Compared to the molecular products obtained where bidentate pyridyl ferrocene ligands behave as chelating moieties with metals,[9b,e,f] ligands **1** and **2** invariably form supramolecular arrays. The wide variety of conformational superstructures seen displays the flexibility of ligand **1** and **2** toward supramolecular construction. The ligands and coordination arrays studied here also exhibit redox activity.

Experimental Section

All reagents and solvents were commercially available except for 1,1′-bis{[1*H*-(2-methyl)imidazol-1-yl]methyl}ferrocene (**2**) and 1,1′-bis[(1*H*-1,2,4-triazol-1-yl)methyl]ferrocene (**1**), which were prepared according to the literature.[10] IR spectra (BioRad FTS 3000 Excalibur series) were obtained using KBr pellets. Elemental analyses were performed by Desert Analytics Laboratory, Tucson, AZ, and the Shanghai Institute of Organic Chemistry.

Cyclic voltammograms were recorded with a Bioanalytical System CV-50w potentiostat. Solid-state voltammograms[9a] were measured by using a carbon-paste working electrode (BAS MF-2010). Well-ground mixtures of each bulk sample and carbon paste (graphite and mineral oil) were set in a cavity on the working

electrode. A carbon counter electrode and a Ag/AgCl reference electrode were used. Measurements were performed by using a three-electrode system in 0.1 mol dm^{-1} NaClO$_4$ aqueous solutions at a scan rate of 0.1 V s^{-1}, in the range −0.3 to 1.2 V.

[Ag{1,1′-bis[(1*H*-1,2,4-triazol-1-yl)methyl]ferrocene}NO$_3$]$_n$ (3). A methanol solution (7 mL) of **1** (35 mg, 0.1 mmol) was slowly layered onto a water solution (3 mL) of AgNO$_3$ (17 mg, 0.1 mmol) in a test tube at room temperature. Complex **3** was obtained as an orange crystalline solid in 2 days (44 mg, 85%). IR (KBr, cm^{-1}): 3092, 3021, 1518, 1351, 1273, 1136, 1026, 987. Anal. Calcd for C$_{16}$H$_{16}$AgFeN$_7$O$_3$: C, 37.10; H, 3.11; N, 18.93. Found: C, 37.16; H, 3.14; N, 19.34.

[Cd{1,1′-bis[(1*H*-1,2,4-triazol-1-yl)methyl]ferrocene}$_2$Cl$_2$]$_n$ (4). Complex **4** was obtained by a procedure similar to that for **3**, except that CdCl$_2$·2.5H$_2$O (11 mg, 0.05 mmol) was used. Product **4** was obtained as an orange crystalline solid in 10 days (34 mg, 77%). IR (KBr, cm^{-1}): 3133, 2970, 1514, 1336, 1271, 1202, 1128, 1011, 978. Anal. Calcd for C$_{32}$H$_{32}$CdCl$_2$Fe$_2$N$_{12}$: C, 43.69; H, 3.67; N, 19.11. Found: C, 43.73; H, 3.67; N, 19.44.

[Zn{1,1′-bis[(1*H*-1,2,4-triazol-1-yl)methyl]ferrocene}Cl$_2$]$_n$ (5). Complex **5** was obtained by a procedure similar to that for **3**, except that ZnCl$_2$ (14 mg, 0.1 mmol) was used. Product **5** was obtained as an orange crystalline solid in 10 days (31 mg, 64%). IR (KBr, cm^{-1}): 3109, 1531, 1445, 1331, 1283, 1204, 1133, 999. Anal. Calcd for C$_{16}$H$_{16}$ZnCl$_2$FeN$_6$: C, 39.67; H, 3.33; N, 17.35. Found: C, 39.59; H, 3.36; N, 17.46.

[Zn[1,1′-bis{[1-(2-methyl)imidazol-1-yl]methyl}ferrocene]-Cl$_2$]$_n$ (6). Complex **6** was obtained by a procedure similar to that for **3** by using ligand **2** (37 mg, 0.1 mmol) with ZnCl$_2$ (14 mg, 0.1 mmol). Product **6** was obtained as an orange crystalline solid in 10 days (35 mg, 69%). IR (KBr, cm^{-1}): 3121, 2928, 1543, 1507, 1421, 1333, 1155, 1038, 1008, 752. Anal. Calcd for C$_{20}$H$_{22}$ZnCl$_2$FeN$_6$: C, 47.05; H, 4.34; N, 10.97. Found: C, 47.27; H, 4.40; N, 10.61.

X-ray Diffraction Studies. Crystals of compound **3**−**6** were removed from the flask and covered with a layer of hydrocarbon oil. A suitable crystal was selected, attached to a glass fiber, and placed in the low-temperature nitrogen stream.[15] Data for **3**−**6** were collected at 86(2) K using a Bruker/Siemens SMART APEX instrument (Mo Kα radiation, $\lambda = 0.71073$ Å) equipped with a Cryocool NeverIce low-temperature device. Data were measured using omega scans of 0.3° per frame, and a full sphere of data was collected for each sample. Exposure times are given in Table 1. A total of 2450 frames were collected with a final resolution of 0.77 Å. The first 50 frames were re-collected at the end of data collection to monitor for decay. Cell parameters were retrieved using SMART[16] software and refined using SAINTPlus[17] on all observed reflections. Data reduction and correction for *Lp* and decay were performed using the SAINTPlus software. Absorption corrections were applied using SADABS.[18] Structures were solved by direct methods and refined by least-squares method on F^2 using the SHELXTL[19] program package. Only compound **3** shows disorder. In this structure, all atoms except the AgNO$_3$ unit were disordered, modeled at 50% occupancy and held isotropic. Only the Fe and AgNO$_3$ atoms were refined anisotropically. All other non-hydrogen atoms in compounds **3**−**6** were refined anisotropically. No decomposition was observed during data collection. Details of the data collection and refinement are provided in Table 1.

(15) Hope, H. *Prog. Inorg. Chem.* **1994**, *41*, 1−49.
(16) *SMART: version 5.625, Bruker Molecular Analysis Research Tool*; Bruker AXS: Madison, WI, 2001.
(17) *SAINTPlus: version 6.22, Data Reduction and Correction Program*; Bruker AXS: Madison, WI, 2001.
(18) *SADABS: version 2.01, An Empirical Absorption Correction Program*; Bruker AXS: Madison, WI, 2001.
(19) *SHELXTL: version 6.10, Structure Determination Software Suite*; Bruker AXS: Madison, WI, 2001.

Supporting Information Available: Crystallographic data in the form of a combined CIF for complexes **3**−**6**. This material is available free of charge via the Internet at http://pubs.acs.org.

OM060327U